Biochemical and Biophysical Research Communications 431 (2013) 203–209

Contents lists available at SciVerse ScienceDirect

Biochemical and Biophysical Research Communications

journal homepage: www.elsevier.com/locate/ybbrc

Tissue factor triggers procoagulation in transplanted mesenchymal stem cells leading to thromboembolism

Kohei Tatsumi [a], Kazuo Ohashi [a,*], Yoshinori Matsubara [b], Ayako Kohori [b], Takahiro Ohno [b], Hiroshi Kakidachi [b], Akihiro Horii [b], Kazuko Kanegae [a], Rie Utoh [a], Takanori Iwata [a], Teruo Okano [a]

[a] Institute of Advanced Biomedical Engineering and Science, Tokyo Women's Medical University, Shinjuku, Tokyo 162-8666, Japan
[b] Corporate R&D Center, Olympus Corporation, Hachioji, Tokyo 192-8512, Japan

ARTICLE INFO

Article history:
Received 20 December 2012
Available online 9 January 2013

Keywords:
Mesenchymal stem cells
Tissue factor
Systemic administration
Thrombosis

ABSTRACT

Mesenchymal stem cells (MSCs) have shown extreme clinical promise as a therapeutic regenerative system in the treatment of numerous types of diseases. A recent report, however, documented lethal pulmonary thromboembolism in a patient following the administration of adipose-derived MSCs (ADSCs). In our study, we designed experiments to examine the role of tissue factor (TF), which is highly expressed at the level of mRNA and localized to the cell surface of cultured MSCs, as a triggering factor in the procoagulative cascade activated by infused MSCs. A high mortality rate of ~85% in mice was documented following intravenous infusion of mouse ADSCs within 24 h due to the observation of pulmonary embolism. Rotation thromboelastometry and plasma clotting assay demonstrated significant procoagulation by the cultured mouse ADSCs, and preconditioning of ADSCs with an anti-TF antibody or usage of factor VII deficient plasma in the assay successfully suppressed the procoagulant properties. These properties were also observed in human ADSCs, and could be suppressed by recombinant human thrombomodulin. In uncultured mouse adipose-derived cells (ADCs), the TF-triggered procoagulant activity was not observed and all mice infused with these uncultured ADCs survived after 24 h. This clearly demonstrated that the process of culturing cells plays a critical role in sensitizing these cells as a procoagulator through the induction of TF expression. Our results would recommend that clinical applications of MSCs to inhibit TF activity using anti-coagulant agents or genetic approaches to maximize clinical benefit to the patients.

1. Introduction

Mesenchymal stem cells (MSCs) are multipotent progenitor cells that are capable of proliferating and differentiating into many different cell lines, including the osteogenic, adipogenic, and chondrogenic lineages [1,2]. Since MSCs were first identified in bone marrow [3], they have been isolated from other various sources including adipose tissue, placenta, umbilical cord blood, lung, and other tissues. Adipose tissue is a particularly appealing resource for MSCs, as it is abundant and easy to procure through minimally invasive procedures [4]. Owing to their multipotency and their immunosuppressive properties, MSCs have extreme potential in the field of tissue engineering, regenerative medicine, and the treatment of immunological disorders [5]. Currently, a large number of MSC-based clinical trials using MSCs are being conducted for the treatment of various diseases worldwide [6].

Nevertheless, animal experimental studies have demonstrated that these cells frequently congregate within the pulmonary circulation after intravenous administration [7,8]. In addition, the clinical application of MSCs has been scrutinized greatly after the intravenous administration of adipose-derived MSCs caused the death of a patient from a pulmonary thromboembolism. Elucidation of the mechanism that causes thrombosis formation following MSCs administration is highly anticipated, since clarification of this process could lead to thrombosis-preventative modifications for the safe advancement in MSC-based therapy.

The aim of this study was to recapitulate the fatal pulmonary embolism events that occurred in the aforementioned clinical case in mouse model [9]. We administered mouse adipose-derived MSCs (mADSCs) to syngeneic mice via the tail vein, and the mortality rates and histological evaluations for MSC-mediated thromboembolism status were assessed. In addition, this study also investigated the precise MSCs-mediated coagulation cascade mechanism that leads to thromboembolism.

Abbreviations: MSCs, mesenchymal stem cells; ADSCs, adipose tissue-derived stem cells; ADCs, adipose tissue-derived cells; TF, tissue factor.

* Corresponding author. Address: Institute of Advanced Biomedical Engineering and Science, Tokyo Women's Medical University, 8-1 Kawada-cho, Shinjuku-ku, Tokyo 162-8666, Japan. Fax: +81 3 3359 6046.
E-mail address: ohashi@abmes.twmu.ac.jp (K. Ohashi).

0006-291X/$ - see front matter © 2013 Elsevier Inc. All rights reserved.
http://dx.doi.org/10.1016/j.bbrc.2012.12.134

2. Materials and methods

2.1. Animals

C57BL/6 wild-type mice (CLEA Japan, Tokyo, Japan), factor IX knock-out (FIX-KO) mice (Jackson Laboratory, Bar Harbor, ME), and green fluorescent protein (GFP)-transgenic mice (Japan SLC, Hamamatsu, Japan) were used. All animal studies were performed in accordance with the institutional guidelines set forth by the Animal Care Committee of Tokyo Women's Medical University.

2.2. Mouse adipose-derived stem cells (mADSCs)

mADSCs were obtained and established from the inguinal adipose tissues of wild-type mice as previously described [10]. In the present studies, mADSCs at passage 3 were used. The cell surface marker pattern of the mADSCs were analyzed by flow cytometry, and found to be identical to that of mesenchymal stem cells (MSCs) ($CD29^+$, $CD44^+$, $CD11^-$, $CD34^-$, and $CD45^-$). The pluripotency of the mADSCs to adipogenic, chondrogenic, and osteogenic lineages were confirmed by Oil Red O, Safranin O, and Alkaline Phosphatase staining, respectively (Supplementary Fig. 1) [10].

2.3. Human MSCs and tissue samples

Three different lots of human ADSCs (hADSCs) and human bone marrow-derived MSCs were purchased from Cellular Engineering Technologies (Coralville, IA). Human periodontal ligament-derived MSCs were obtained from the extracted wisdom teeth from three healthy volunteer donors acquiring a written informed consent for the experimental use [11]. Normal human liver tissues were obtained from surgically excised liver specimens after acquiring a written informed consent for the experimental use of harvested liver samples. Hepatocytes were isolated by a two-step collagenase perfusion method [12].

2.4. mADSCs infusion into mice

The cultured mADSCs were harvested as a single cell suspension by trypsinization, re-suspended and infused into syngenic mice at a volume of 200 μL via tail vein using a 27-gauge needle as slowly as possible (about 1 min). The several organs were isolated immediately after death, their appearances were grossly examined, and then fixed in paraffin for histological sectioning and analysis following hematoxylin and eosin (H&E) staining. To localize the infused GFP-positive donor cells, the thoracic cavity was opened immediately after death and observed using *in vivo* imaging system OV110 (Olympus, Tokyo, Japan). The images were acquired with a 0.56× objective lens at 100 μm step in the z-direction, and merged into a single image with the use of OV110 software (Olympus).

2.5. Rotation thromboelastometry (ROTEM)

Citrated whole blood was collected from wild-type mice or healthy human volunteers. Aliquots of whole blood (90 μL) were transferred to a pre-warmed (37 °C) ROTEM mini cup, and 10 μL of cell suspension or PBS were mixed (final conc. 7.5×10^4 cells/mL, mimicking the *in vivo* administration experiment in Fig. 1). After 10 min incubation, 7 μL of 0.2 M $CaCl_2$ was added to initiate the reaction (Tem Innovations, Munich, Germany). Parameters assessed were clotting time (CT), clot formation time (CFT), maximum clot firmness (MCF), and alpha-angle [13].

2.6. Clotting assays

Mouse blood samples were immediately anticoagulated with 0.1 vol. of 3.8% sodium citrate (Sysmex, Kobe, Japan) and centrifuged. Plasma clotting time was measured using KC4 Delta Coagulometer (Trinity Biotech, Wicklow, Ireland). In brief, 50 μL of plasma mixed with 100 μL of ADSCs suspension was pre-incubated at 37 °C for 5 min. Then, 50 μL of 0.02 M $CaCl_2$ was added to the reaction mixture to measure the clotting times. In each experiment, the clotting time were converted into the TF unit based on the standard curve, which was drawn from the clotting time of one-tenth serially-diluted rat brain-derived TF reagent (ThromboCheck PT Plus, Sysmex). The value of undiluted solution was defined as 10,000 TF units. Normal mouse plasma and factor IX (FIX)-deficient plasma were obtained from wild-type and FIX-KO mice, respectively. Factor VII (FVII)-deficient plasma was isolated from wild-type mice intravascularly injected with *F7* siRNA (Supplementary Fig. 2). Normal human plasma (Coagtrol N), human FIX-deficient plasma (ThromboCheck factor IX), and human FVII-deficient plasma (ThromboCheck factor VII) were purchased from Sysmex. For tissue factor (TF) inhibition assay, isolated mADSCs were incubated with several amounts of rabbit anti-mouse TF IgG (American Diagnostica, Stamford, CT) for 20 min at room temperature. A clotting assay was performed using NMP mixed with the mADSCs incubated with the TF IgG. As a negative control, normal rabbit IgG (R&D Systems, Minneapolis, MN) was used. The range of antibody concentration tested in our experiment was 0–6000 pg/cell.

2.7. Immunofluorescence cell staining and flow cytometry for TF

mADSCs or hADSCs dispersed from culture dishes were stained for mouse or human TF using rabbit anti-mouse TF IgG (100 μg/mL; American Diagnostica) or purified mouse anti-human CD142 (Becton Dickinson, Franklin Lakes, NJ), respectively. The appropriate secondary antibodies labels with Alexa-Fluor-488 (10 μg/mL; Molecular Probes, Eugene, OE) were used at 4 °C for 1 h. For immune staining, the nuclei were visualized with 4′,6-diamino-2-phenylindole reagents (ProLong® Gold Antifade Reagent with DAPI, Molecular Probes), and the images were taken with FV10i (Olympus). For flow cytometry, FACSAria™ (Becton Dickinson) were utilized and the obtained results were analyzed using FlowJo (Tree Star, Ashland, OR). As a negative control, normal rabbit IgG (R&D Systems) and normal mouse IgG (Santa Cruz Biotechnology, Santa Cruz, CA) were reacted with mADSCs and hADSCs, respectively.

2.8. RT-PCR

Total RNA were extracted from cell samples and cDNA were synthesized from the RNA [14]. The first-strand cDNA samples were subjected to PCR amplification in the StepOnePlus Real-Time PCR Systems (Life Technologies Japan, Tokyo, Japan) followed by 3% agarose gel electrophoresis. The gene expression levels of TF (*F3*) and FSAP (*Habp2*) were normalized to the housekeeping gene, β-actin (*Actb*). The PCR probe and primers were purchased from Applied Biosystems (TaqMan Gene Expression Assay, Assay ID: Mm00438853_m1 for mouse TF, Mm00525028_m1 for mouse FSAP, Mm00607939_s1 for mouse β-actin, Mm99999915_g1 for mouse GAPDH, Hs01076032_m1 for human TF, Hs00188053_m1 for human FSAP, Hs99999905_m1 for human GAPDH, and Hs99999903_m1 for human β-actin).

2.9. Generation of mADSCs sheets

mADSCs cells were cultured on 35-mm temperature-responsive culture dishes (UpCell®; CellSeed, Tokyo, Japan) [12]. After ADSCs

A

Number of injected ADSCs	Total mouse number	Number of survived mice (24 h)	Survival rate (%)
1.5×10^5 cells / mouse	13	2	15
1.5×10^4 cells / mouse	10	10	100
0 cells, PBS only / mouse	10	10	100

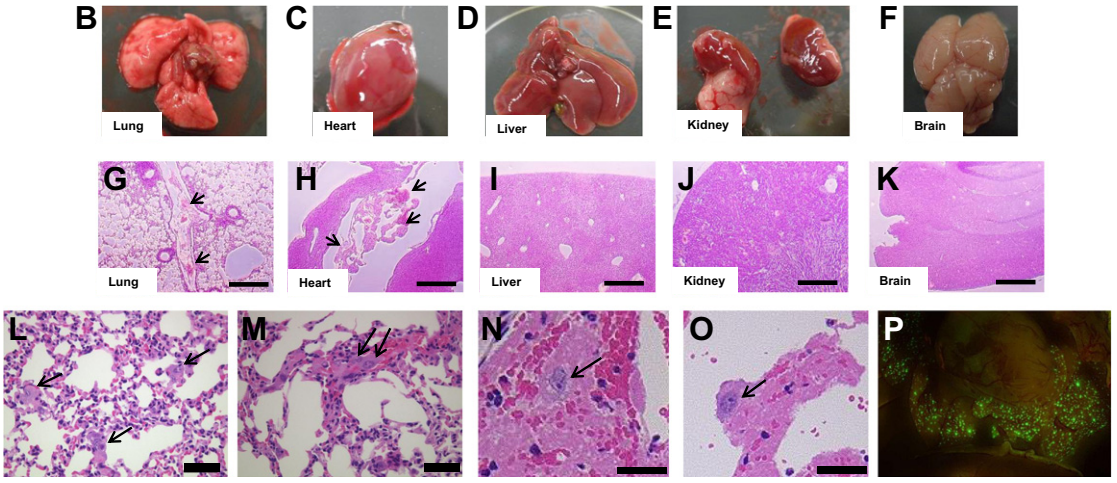

Fig. 1. Survival and histological examination of the mice that died after receiving intravenous administration of mADSCs. Two different number of mouse adipose-derived MSCs (mADSCs) were administered to syngeneic wild-type C57BL/6 mice via tail vein. (A) The survival rate of recipient mice at 24 h after mADSCs administration. (B–O) Mouse organ analysis following death after mADSCs administration. The following organs were analyzed, the lung (B and G), heart (C and H), liver (D and I), kidney (E and J), and brain (F and K). Gross appearance (B–F) and H&E staining (G–K) of the excised organs are shown, respectively. Arrows denote fibrin clots formed in pulmonary artery of the lung (G) and right ventricle of the heart (H). Scale bars = 500 μm. (L and M) Arrows denote administered mADSCs trapped in the alveolar walls (L) and the peripheral pulmonary arteries (M). Note that mADSCs were wrapped by fibrin clots. Scale bars = 50 μm. (N and O) Arrows denote administered mADSCs with fibrin clots located in right ventricle of the heart. Scale bars = 20 μm. (P) The fluorescence gross appearance of recipient lungs that were infused with GFP-positive ADSCs.

reached full confluency, the culture temperature was lowered to 20 °C for 30 min allowing the natural cell detachment from the culture surface and enabling for the harvesting of the cells as a monolayer sheet.

2.10. Antithrombotic effects of thrombomodulin on hADSCs

Recombinant human thrombomodulin (Recomodulin™) was purchased from Asahi Kasei Pharma (Tokyo, Japan). Human citrated whole blood or normal human plasma (Coagtrol) inoculated with thrombomodulin was mixed with hADSCs for ROTEM analysis or plasma clotting assay. The final concentration of exogenously added thrombomodulin in the whole blood or plasma samples was between 0 and 100 μg/mL.

2.11. Statistical analyses

Significant differences were tested by Mann-Whitney *U*-test between unpaired groups. *P* value of <0.05 was considered to be significant. All data were presented as the mean ± s.e.m.

3. Results and discussion

To evaluate the risk of intravenous injection of ADSCs, 1.5×10^5 cells of the mADSCs were administered to syngeneic wild-type C57BL/6 mice via tail vein. This intravenously-administered cell number per body weight is nearly identical to the previously reported clinical studies [15,16]. Within 24 h after injection, the mortality rate of the mice was nearly 85% (Fig. 1A). When PBS or 1.5×10^4 of mADSCs were administered, the mice showed no adverse events and survived. Histological assessment of the mice revealed multiple fibrin clots formed in the right ventricle and pulmonary arteries. Infused mADSCs were found in the core of the fibrin clots (Fig. 1N and O). Liver sinusoids around hepatic vein were slightly enlarged, indicating the stagnation of venous return flow. No remarkable pathological change was observed in the kidney ruling out the possibility of systemic intravascular hypercoagulation. These results indicate that administered mADSCs triggered thrombus formation around the cells, and initiated pulmonary embolism immediately after the administration (Fig. 1B–O). Further, infused ADSCs were clearly demonstrated to be stacked in the lungs when GFP-transgenic mice-derived ADSCs were used as donor cells (Fig. 1P). These data prompted us to further investigate the mechanisms for ADSCs infusion-related thromboembolism.

To investigate the procoagulant property of mADSCs in detail, we first performed ROTEM using citrated mouse whole-blood and mADSCs. The re-calcified whole blood samples mixed with mADSCs (final conc. 7.5×10^4 cells/mL mimicked the *in vivo* experiment mentioned above) demonstrated significant reduction in the CT and CFT, and increased alpha-angle compared with the control samples mixed with PBS (Fig. 2A–D). The increasing tendency of the coagulation property in CFT was observed during the incubation period as the single cell suspensions became longer after mADSCs were harvested from culture dishes (Fig. 2E–H). These results indicated that mADSCs possessed a significant procoagulant property against whole blood, and this property will be enhanced during cell suspension period. Next, we investigated clotting times

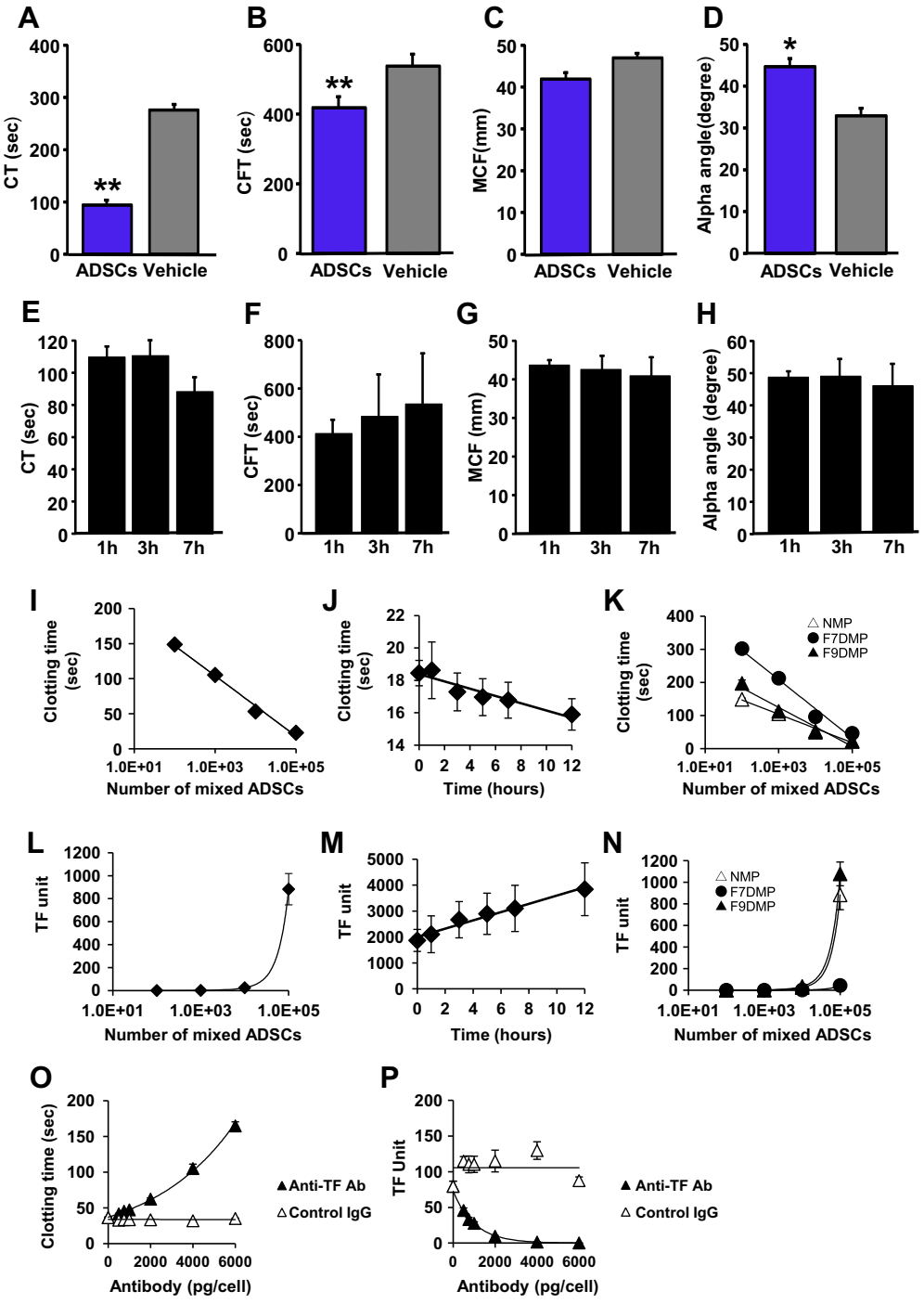

Fig. 2. Assessment of procoagulant property of mADSCs. (A–D) Representative parameters of ROTEM assay using mADSCs and mouse whole blood ($n = 5$). Final concentration of mixed mADSCs was 7.5×10^4 cells/mL. Analyzed parameters were (A) clotting time (CT), (B) clot formation time (CFT), (C) maximum clot firmness (MCF), and (D) alpha-angle. (E–H) ROTEM assay was performed using mADSCs that were kept as a single cell suspension in PBS at room temperature for 1, 3, and 7 h after cell harvesting. Final concentration of mixed mADSCs was 7.5×10^4 cells/mL ($n = 3$ for each group). (I–P) Clotting assays using different mouse plasma and mADSCs. (I) Clotting times of pooled normal mouse plasma (NMP) mixed with mADSCs. (J) Clotting times of NMP mixed with mADSCs (1.0×10^5 cells) at different times after cell harvesting. Cell viabilities of mADSCs at the time of assay were 96.0 ± 0.0%, 96.5 ± 2.0%, 95.2 ± 0.3%, 95.9 ± 0.2%, 95.5 ± 0.8%, and 94.1 ± 2.3%, at 0, 1, 3, 5, 7 and 12 h of suspension, respectively. (K) Clotting assay using NMP, factor VII-deficient mouse plasma (F7DMP), or factor IX-deficient mouse plasma (F9DMP) with mADSCs. (L–N) The clotting times recorded in (I–K) were converted into the arbitrary TF units. (O and P) Clotting assay using NMP with mADSCs which were preincubated with several concentrations of anti-TF monoclonal antibody (filled triangles) or control IgG antibody (open triangles) ($n = 3$ for each group). $^*P < 0.05$ and $^{**}P < 0.01$ vs. vehicles. All values were expressed as the mean ± s.e.m.

by mixing normal mouse plasma (NMP) with various numbers of mADSCs. The clotting times were shortened in a cell number-dependent manner (Fig. 2I). Clotting time shortening was also dependent on the length of the incubation period as a single cell suspension (Fig. 2J). This indicates that mADSCs have a significant procoagulant property against plasma as well as whole blood, and the clot formations by mADSCs are mediated by some factor(s) in the plasma.

Subsequently, we set out an experiment to identify the responsible factor(s) in plasma. To achieve this goal, we prepared factor

IX-deficient mouse plasma (F9DMP) and factor VII-deficient mouse plasma (F7DMP) (Supplementary Fig. 2), and performed clotting assays. The clotting times of NMP and those of F9DMP were nearly identical. In marked contrast, when F7DMP were used, the clotting time was found to be significantly prolonged compared with those of NMP or F9DMP (Fig. 2K). These results clearly suggested that mADSCs-derived procoagulant activities may activate the extrinsic coagulation pathway through TF, since factor VII acts as a factor of extrinsic pathway and be mainly activated by TF. After converting the recorded times to the arbitrary TF units as described in materials and methods, the time-dependency of the procoagulant activity and the discrepancy among the three types of plasma were clearly observed (Fig. 2L–N). To further confirm the central role of TF in the mADSC-mediated hypercoagulation, mADSCs were preconditioned with several concentrations of anti-TF monoclonal antibody, followed by clotting time measurement using NMP. The procoagulant properties were clearly suppressed in an antibody concentration-dependent manner (Fig. 2O and P).

From above results, we assumed that TF is strongly expressed on the cell surface of mADSCs and triggers the blood coagulation. To confirm this, fluorescent immunostaining, flow cytometry, and RT-PCR for TF were conducted using mADSCs. TF was strongly expressed around mADSCs surfaces by immunostaining and flow cytometry (93.73% of mADSCs was TF-positive) (Fig. 3A–C). Significant mRNA expression levels of *TF* gene were observed in mADSCs by RT-PCR (Fig. 3D and E). Factor seven activating protease (FSAP), another candidate plasma protein encoded by *Habp2* and has been shown to activate factor VII [17], was nearly undetectable in the mADSCs (Fig. 3F). These results taken together indicated that the responsible factor that accelerates mADSC-mediated blood coagulation is TF expressed on the cellular surfaces.

Next, we investigated whether human MSCs also possess strong coagulation properties. We prepared commercially available human ADSCs (hADSCs) lines, and evaluated their abilities for facilitating blood coagulation by ROTEM and plasma clotting assay. ROTEM demonstrated significant shortening of CT and CFT, and increased alpha-angle compared with the control samples mixed with PBS (Fig. 4A–D). The values of clotting time were remarkably shortened in hADSCs number-dependent manner when normal human plasma was mixed with hADSCs. Same findings were also observed when factor IX-deficient plasma was used. However, the shortened clotting time was not observed when factor VII-deficient plasma was used (Fig. 4E and F). hADSCs were strongly stained with human TF antibody (Fig. 4G and H). Flow cytometry demonstrated that more than 97% of cells were positive for human TF (Fig. 4I). Strong expressions of human TF mRNA and no expression of human FSAP mRNA were detected by RT-PCR in hADSCs samples (Fig. 4J–L). The accelerated procoagulant activities detected by ROTEM and clotting assay were also observed in other types of human MSCs including bone marrow-derived and periodontal ligament-derived MSCs. Taken together, human MSCs, including hADSCs, strongly expressed TF protein around their cell surfaces, resulting in the triggering systemic blood coagulation by accelerating the extrinsic blood coagulation pathway.

As described above, ADSCs tended to increase TF expression in a time-dependent manner after being harvested from culture dishes by trypsinization. We hypothesized that induction of TF expression on ADSCs is evoked when they lose contact with surrounding cells. To test this, we compared the TF mRNA expression levels of mADSCs in suspension and mADSCs in cell sheet format. In an attempt to amplify the difference of TF expression of both ADSC formats, the cells were kept in suspension at room temperature for 1, 3, and 5 h, followed by RNA extraction. No statistical differences of TF

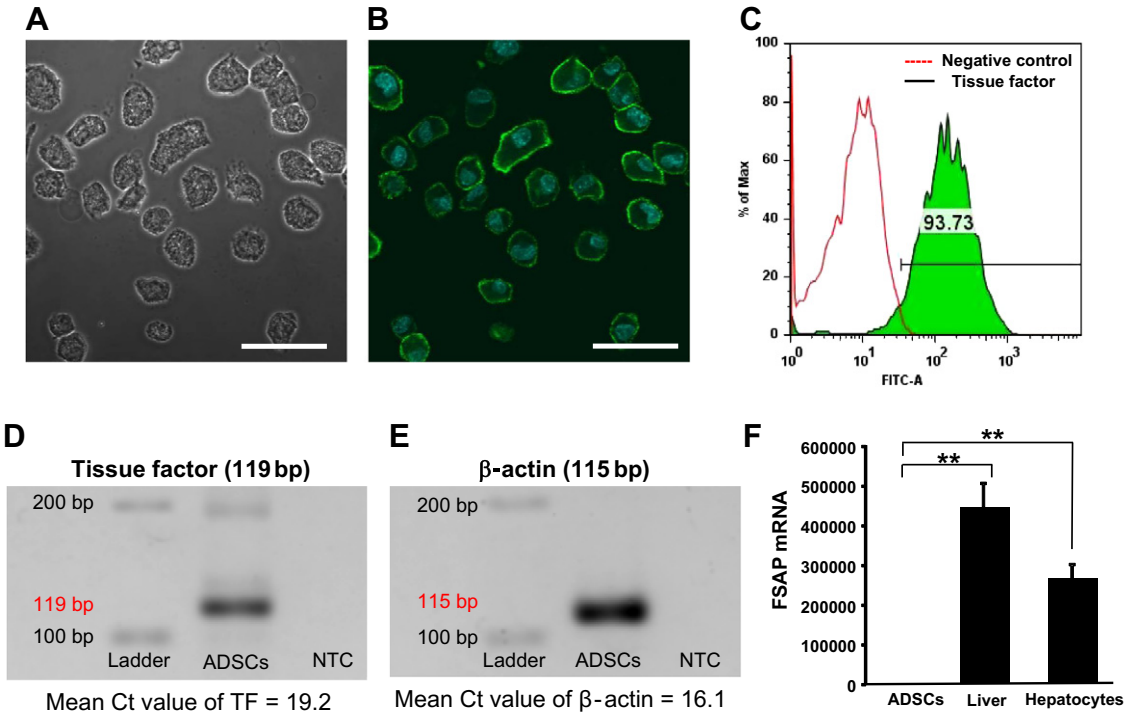

Fig. 3. Tissue factor (TF) expression on mADSCs. (A and B) Immunostaining for mouse TF on mADSCs. Nuclei were visualized with DAPI. (A) Bright field. (B) Fluorescence (green, TF; and blue, nucleus). Note that strong TF signals were detected on cell surface of the mADSCs. Scale bars = 50 μm. (C) Flow cytometric assessment for mouse TF on mADSCs. mADSCs that were reacted negative control antibody (normal rabbit IgG) did not show any fluorescence signals. (D and E) RT-PCR for mouse TF in mADSCs. The amplicon lengths were 119 bp and 115 bp for mouse TF (D) and mouse β-actin (E), respectively. NTC; no template control. (F) The gene expression of FSAP (*Habp2*) in mADSCs. First-strand cDNA of mADSCs, mouse liver tissues, and primary mouse hepatocytes were subjected to RT-PCR for FSAP (*Habp2*), and normalized to their levels of housekeeping gene (β-actin) expression. The expression levels were shown as relative values compared with mADSCs samples ($n = 3$, each group). $^{**}P < 0.01$.

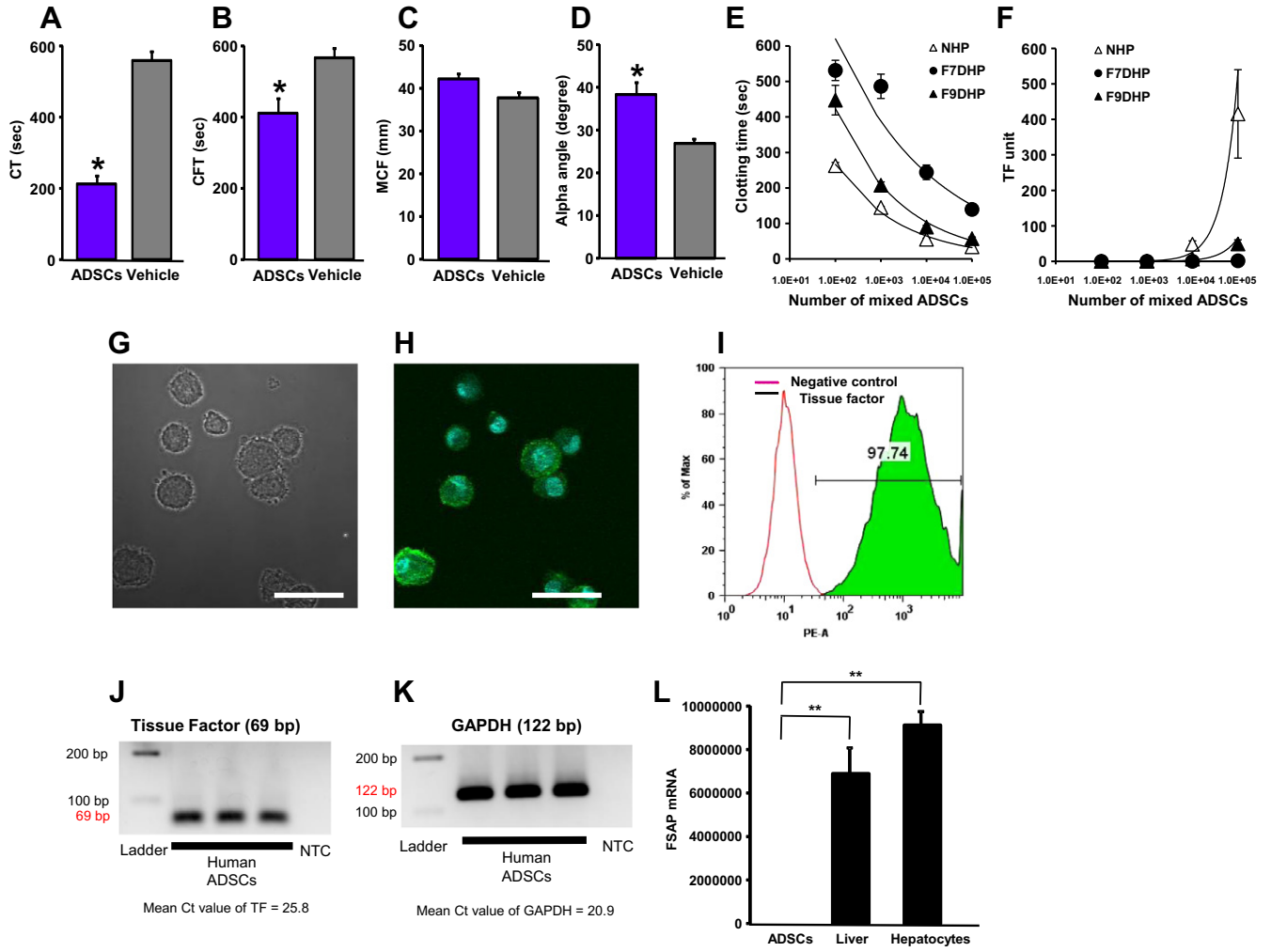

Fig. 4. Assessment of TF-triggered procoagulant property of human ADSCs. (A–D) ROTEM assay using human ADSCs (hADSCs) and human whole blood ($n = 3$). Analyzed parameters were: (A) CT, (B) CFT, (C) MCF, and (D) alpha-angle. $^{*}P < 0.05$ vs. vehicles. (E) Clotting assay using normal human plasma (NHP), factor VII-deficient human plasma (F7DHP), or factor IX-deficient human plasma (F9DHP) with hADSCs ($n = 3$, each group). (F) The clotting times recorded in (E) were converted into arbitrary TF units. (G and H) Immunostaining for human TF on hADSCs. (G) Bright field. (H) Fluorescence (green; TF, and blue; nucleus). Scale bars = 50 μm. (I) Flow cytometric assessment for human TF on hADSCs. (J and K) RT-PCR for human TF of hADSCs. The amplicon lengths were 69 bp and 122 bp for human TF (J) and human GAPDH (K), respectively. NTC; no template control. (L) The gene expression of FSAP (*Habp2*) in hADSCs. First-strand cDNA of hADSCs, human liver tissues, and primary human hepatocytes were subjected to RT-PCR for FSAP (*Habp2*), and normalized to their levels of housekeeping gene (β-actin) expression. The expression levels were shown as relative values compared with hADSCs samples ($n = 3$, each group). $^{**}P < 0.01$.

mRNA expression between the two groups were observed, indicating that TF had been highly expressed during the culture period (Supplementary Fig. 3).

To minimize TF-triggered intravascular coagulation, it could be reasonably speculated that the use of anti-coagulant agents would be feasible. In this study, we focused on the use of recombinant human thrombomodulin (rhTM) as a potential anticoagulant agent [18]. After normal human whole blood or plasma samples with rhTM were mixed with hADSCs, ROTEM and clotting assay were performed. ADSC-triggered procoagulation were dramatically suppressed in rhTM concentration-dependent manner (Supplementary Fig. 4), which provides strong feasibility in the use of rhTM during the infusion of MSCs injection therapy.

Recently, uncultured adipose-derived cells (ADCs), freshly digested from adipose tissue consisting heterogeneous cell populations, have been highlighted as an alternative feasible cell source for regenerative medicine [6]. Mouse ADCs (mADCs) were freshly isolated from adipose tissue of wild-type mice and analyzed without cell culturing. Unlike the case with mADSCs, *in vitro* coagulation assay clarified that mADCs had almost no coagulant activity (Supplementary Fig. 5). TF were barely detected on the cell surface of mADCs by immunostaining, and TF mRNA expression in mADCs was only one-tenth of that in mADSCs. And, *in vivo* transplantation experiments, in which mADSCs were injected to mice intravenously (1.5×10^5 cells/mouse), caused neither death nor remarkable histological changes in any organs after intravenous administration.

In conclusion, our study confirms that TF has a critical role in promoting MSCs-mediated coagulation in living animals, and that its expression is likely to lead to thromboembolism and subsequent death of a patient treated with MSCs. From our study, it is clear that additional interventions are required to weaken the activation of the coagulation pathway that is mediated by cultured MSCs, and new clinical protocols that incorporate the administration of generic anticoagulants or even, more specifically, genetic inhibitors toward TF must be developed. As an alternative method, tissue engineering approaches that allow engraftment of MSCs at local spots would be recommended, since these methods would reduce the likelihood of MSCs-associated thromboembolism in the transplanted patients.

Acknowledgments

This study was partially supported by Creation of innovation centers for advanced interdisciplinary research areas Program in the Project for Developing Innovation Systems "Cell Sheet Tissue Engineering Center (CSTEC)" from the Ministry of Education, Culture, Sports, Science and Technology (MEXT), Japan. The authors would like to thank Dr. Frank Park (Medical College of Wisconsin) for his critical reading of the manuscript.

Appendix A. Supplementary data

Supplementary data associated with this article can be found, in the online version, at http://dx.doi.org/10.1016/j.bbrc.2012.12.134.

References

[1] M. Dominici, K. Le Blanc, I. Mueller, I. Slaper-Cortenbach, F. Marini, D. Krause, R. Deans, A. Keating, D. Prockop, E. Horwitz, Minimal criteria for defining multipotent mesenchymal stromal cells. The International Society for Cellular Therapy position statement, Cytotherapy 8 (2006) 315–317.
[2] M.F. Pittenger, A.M. Mackay, S.C. Beck, R.K. Jaiswal, R. Douglas, J.D. Mosca, M.A. Moorman, D.W. Simonetti, S. Craig, D.R. Marshak, Multilineage potential of adult human mesenchymal stem cells, Science 284 (1999) 143–147.
[3] A.J. Friedenstein, K.V. Petrakova, A.I. Kurolesova, G.P. Frolova, Heterotopic of bone marrow. Analysis of precursor cells for osteogenic and hematopoietic tissues, Transplantation 6 (1968) 230–247.
[4] P.A. Zuk, M. Zhu, H. Mizuno, J. Huang, J.W. Futrell, A.J. Katz, P. Benhaim, H.P. Lorenz, M.H. Hedrick, Multilineage cells from human adipose tissue: implications for cell-based therapies, Tissue Eng. 7 (2001) 211–228.
[5] S. Bajada, I. Mazakova, J.B. Richardson, N. Ashammakhi, Updates on stem cells and their applications in regenerative medicine, J. Tissue Eng. Regen. Med. 2 (2008) 169–183.
[6] H. Mizuno, Adipose-derived stem and stromal cells for cell-based therapy: current status of preclinical studies and clinical trials, Curr. Opin. Mol. Ther. 12 (2010) 442–449.
[7] D. Furlani, M. Ugurlucan, L. Ong, K. Bieback, E. Pittermann, I. Westien, W. Wang, C. Yerebakan, W. Li, R. Gaebel, R.K. Li, B. Vollmar, G. Steinhoff, N. Ma, Is the intravascular administration of mesenchymal stem cells safe? Mesenchymal stem cells and intravital microscopy, Microvasc. Res. 77 (2009) 370–376.
[8] J. Gao, J.E. Dennis, R.F. Muzic, M. Lundberg, A.I. Caplan, The dynamic in vivo distribution of bone marrow-derived mesenchymal stem cells after infusion, Cells Tissues Organs 169 (2001) 12–20.
[9] D. Cyranoski, Korean deaths spark inquiry, Nature 468 (2010) 485.
[10] K. Ohashi, Y. Matsubara, K. Tatsumi, A. Kohori, R. Utoh, H. Kakidachi, A. Horii, M. Tsutsumi, T. Okano, Cell therapy using adipose derived stem cells for chronic liver injury in mice, Cell Med. 3 (2012) 113–119.
[11] T. Iwata, M. Yamato, Z. Zhang, S. Mukobata, K. Washio, T. Ando, J. Feijen, T. Okano, I. Ishikawa, Validation of human periodontal ligament-derived cells as a reliable source for cytotherapeutic use, J. Clin. Periodontol. 37 (2010) 1088–1099.
[12] K. Ohashi, T. Yokoyama, M. Yamato, H. Kuge, H. Kanehiro, M. Tsutsumi, T. Amanuma, H. Iwata, J. Yang, T. Okano, Y. Nakajima, Engineering functional two- and three-dimensional liver systems in vivo using hepatic tissue sheets, Nat. Med. 13 (2007) 880–885.
[13] R.J. Luddington, Thrombelastography/thromboelastometry, Clin. Lab. Haematol. 27 (2005) 81–90.
[14] K. Tatsumi, K. Ohashi, S. Taminishi, Y. Sakurai, K. Ogiwara, A. Yoshioka, T. Okano, M. Shima, Regulation of coagulation factors during liver regeneration in mice. mechanism of factor VIII elevation in plasma, Thromb. Res. 128 (2011) 54–61.
[15] M. Duijvestein, A.C. Vos, H. Roelofs, M.E. Wildenberg, B.B. Wendrich, H.W. Verspaget, E.M. Kooy-Winkelaar, F. Koning, J.J. Zwaginga, H.H. Fidder, A.P. Verhaar, W.E. Fibbe, G.R. van den Brink, D.W. Hommes, Autologous bone marrow-derived mesenchymal stromal cell treatment for refractory luminal Crohn's disease: results of a phase I study, Gut 59 (2010) 1662–1669.
[16] O. Honmou, K. Houkin, T. Matsunaga, Y. Niitsu, S. Ishiai, R. Onodera, S.G. Waxman, J.D. Kocsis, Intravenous administration of auto serum-expanded autologous mesenchymal stem cells in stroke, Brain 134 (2011) 1790–1807.
[17] J.J. Sidelmann, S.O. Skouby, C. Kluft, U. Winkler, F. Vitzthum, H. Schwarz, J. Gram, J. Jespersen, Plasma factor VII-activating protease is increased by oral contraceptives and induces factor VII activation in vivo, Thromb. Res. 128 (2011) e67–72.
[18] W. Cui, J.T. Wilson, J. Wen, J. Angsana, Z. Qu, C.A. Haller, E.L. Chaikof, Thrombomodulin improves early outcomes after intraportal islet transplantation, Am. J. Transplant. 9 (2009) 1308–1316.